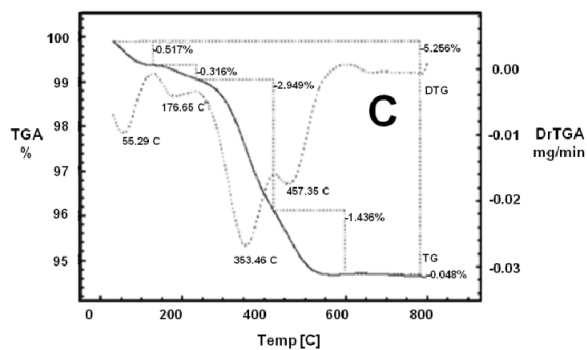
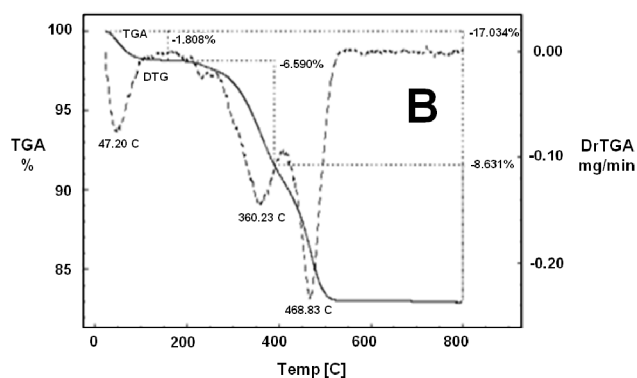
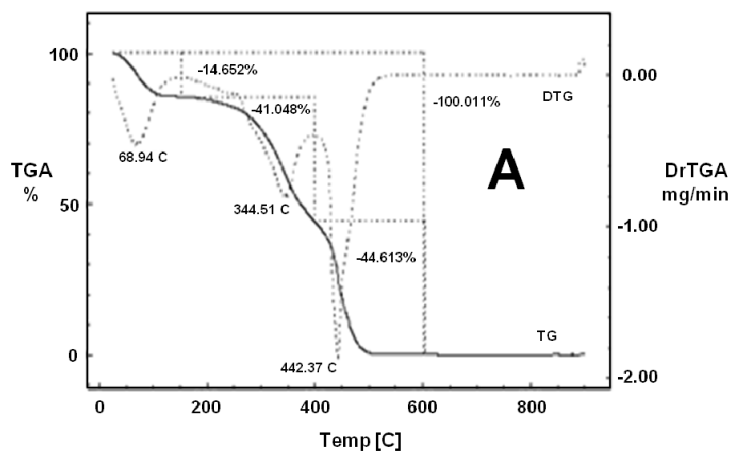


Supplemental Material

Thermogravimetric analysis

The thermal behaviour of the TiO₂ NP, cytochrome *c*-containing TiO₂ NP, titanate nanotubes, and the cytochrome *c*-containing titanate nanotubes investigated using thermogravimetry is shown in Figs. 1S A, B, C, D, and E. The Figures are discussed in the main text of the article.



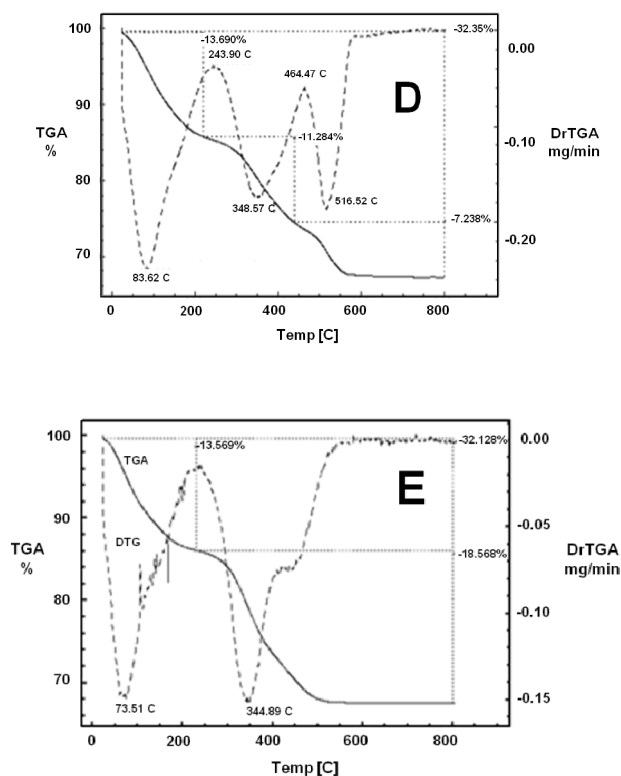


Fig. 1S. TGA–DTG curves obtained under a nitrogen atmosphere (60 mL min^{-1}) using a sample mass between 4–6 mg in the range from room temperature to $800 \text{ }^\circ\text{C}$ with a maximum heating rate of $10 \text{ }^\circ\text{C min}^{-1}$. (A) $20 \text{ } \mu\text{M}$ cytochrome *c* solution. (B) Physical mixture of cytochrome *c* and TiO_2 NP. (C) $20 \text{ } \mu\text{M}$ cytochrome *c* solution incubated with 0.5 mg/mL TiO_2 NP in a 5 mM phosphate buffer (pH 8.0) under irradiation with a 125 W UV lamp. (D) Physical mixture of cytochrome *c* and titanate nanotubes. (E) $20 \text{ } \mu\text{M}$ cytochrome *c* solution incubated with 0.5 mg/mL titanate nanotubes in a 5 mM phosphate buffer (pH 8.0) under irradiation with a 125 W UV lamp.

Mechanism of cytochrome c reduction by titania nanostructures

Hydroxyl radical generated during irradiation of TiO_2 NP was detected by the EPR spin-trap technique by using DMPO to determine the nature of the reactive oxygen species generated in the TiO_2 NP suspension under UV irradiation.

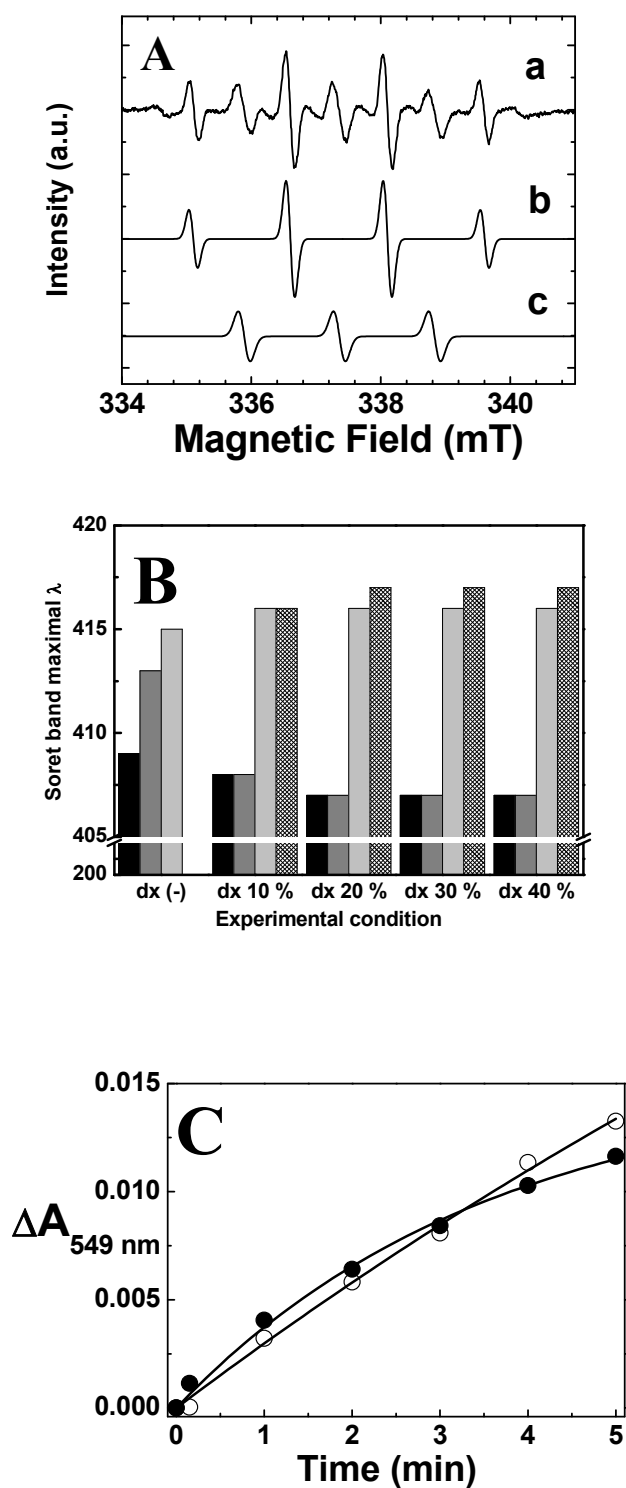


Fig. 2S. Mechanism of cytochrome *c* reduction by TiO₂ NP. (A) EPR spectra of DMPO adducts obtained during the irradiation of TiO₂ NP. (B) Photo-reduction of 20 μ M cytochrome *c* assessed by the red shift of the Soret band peak under the following conditions: 5 mM phosphate buffer, pH of 8.0 (black columns), plus TiO₂ NP (gray columns), plus β -mercaptoethanol (light gray columns), and plus both TiO₂ NP and β -mercaptoethanol (densely patterned columns). The experiments were assayed in the absence and in the presence of 10, 20, 30, and 40% dioxane as indicated on the graph. (C) Kinetics of cytochrome *c* reduction by TiO₂ NP in an aqueous medium (white circles) and in deuterated water (black circles). The results are representative of a set of three independent experiments, and the standard deviation error was always lower than 10%.

The irradiation of the TiO₂ NP suspension in the absence of cytochrome *c* led to the appearance of detectable EPR adduct signals (Fig. 2SA, line *a*). The simulation of the DMPO adducts presented hyperfine coupling constants $a^N =$

$a^H = 15$ G and lw (line width) = 1.35 (Fig. 2SA, line *b*) that could be assigned to the DMPO/ \cdot OH adduct [1, 2] and $a^N = 14.7$ G, and $lw = 1.85$ G (Fig. 2SA, line *c*) whose origin and identity remain to be elucidated. The unidentified adduct corresponded to a DMPO adduct with α hydrogen substituted for a group unable to establish hyperfine splitting. The persistence of a DMPO/ \cdot OH adduct signal in the absence of oxygen corroborated that the free radical resulted from water photolysis and the DMPO adduct did not result from the reaction with singlet oxygen (not shown). No such signals were detected in the dark. This means that irradiation is essential for the generation of \cdot OH on the surface of the catalyst. As expected, the DMPO/ \cdot OH adduct signal was not detected after the irradiation of the TiO_2 NP suspensions incubated with cytochrome *c*. Considering the high reactivity of \cdot OH, we could explain this result explained by the trapping of the free radical by the cytochrome *c* molecules adsorbed on the TiO_2 NP surface. The photo-induced electron transfer from water to cytochrome *c* mediated by the TiO_2 NP was also probed by changing the dielectric constant of the medium (Fig. 2SB) and by replacing water with D_2O (Fig. 2SC). Fig. 2SB shows the degree of the Soret band red shift exhibited by cytochrome *c* challenged by the reducing action of the TiO_2 NP and β -mercaptoethanol at the different percentages of dioxane. The presence of 20% dioxane in the medium was sufficient to completely prevent the reduction of cytochrome *c* by the TiO_2 NP (gray bars), but even 40% dioxane had no effect on the chemical reduction of cytochrome *c* by β -mercaptoethanol (light gray bars). The impairment of cytochrome *c* reduction by the TiO_2 NP promoted by dioxane was not due to the damage in the protein promoted by the TiO_2 NP in the presence of the solvent, since cytochrome *c* not reduced by TiO_2 NP in the presence of dioxane was promptly reduced after the addition of β -mercaptoethanol (dense pattern bars). Fig. 2SC shows the kinetics of cytochrome *c* reduction by the TiO_2 NP irradiated in water (open circles) and in D_2O (closed circles), in an argon atmosphere. The replacement of water by D_2O increased by fivefold the rate of cytochrome *c* reduction by the TiO_2 NP as compared to water as the reducing agent for cytochrome *c*. In the case of the TiO_2 NP/cytochrome *c* system, it is reasonable to assume that the classical mechanism of semiconductors is involved in the reduction of the heme iron of cytochrome *c* freely in the solution.

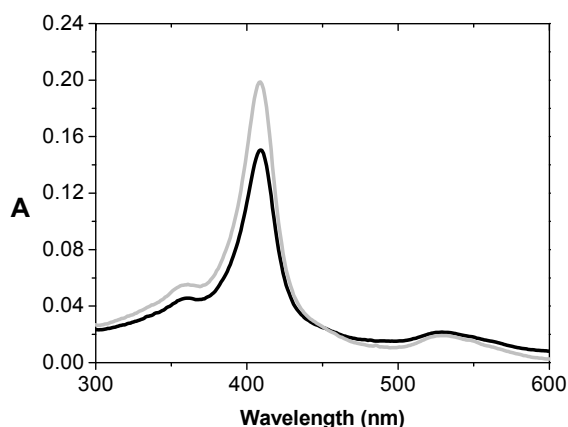


Fig. 3S. Electronic absorption spectra of native cytochrome *c* (light gray line) and cytochrome *c* desorbed from titanate nanotubes (black line). The experiments were carried out as described in Materials and Methods.

However, in the case of the titanate nanotubes/cytochrome *c*, considering that cytochrome *c* was completely oxidized when desorbed from the nanotubes, even when the procedure was performed in an argon atmosphere (Fig. 3S), we concluded that the mechanism remains to be elucidated.

References

1. J. Aron, D.A. Baldwin, H.M. Marques, J.M. Pratt and P.A. Adams, *J. Inorg. Biochem.*, 1986, **27**, 227.T.
2. Prieto, R.O. Marcon, F.M. Prado, A.C.F. Caires, P. Di Mascio, S. Brochsztain, O.R. Nascimento and I.L. Nantes, *Phys. Chem. Chem. Phys.*, 2006, **8**, 1963.